Unveiling the Impact of PET Method Selection on Trends in Hydrological Cycle Components Across Europe

Vishal Thakur[1], Yannis Markonis[1], Rohini Kumar[2], Johanna Ruth Thomson[1], Mijael Rodrigo Vargas Godoy[1,3], Martin Hanel[1], and Oldrich Rakovec[1,2]

[1] Faculty of Environmental Sciences, Czech University of Life Sciences Prague, Kamýcká 129, Praha – Suchdol, Czech Republic

[3]River-Coastal Science & Engineering, Tulane University, New Orleans, 70118, Louisiana, USA

[2]Department Computational Hydrosystems, UFZ-Helmholtz Centre for Environmental Research, Leipzig, Germany

Correspondence: Vishal Thakur (thakur@fzp.czu.cz)

Text S1. Citation Statements

This section presents the original excerpts from the research articles utilized in our study. We excluded citations for the datasets, models, and PET method formulations. We organize the excerpts alphabetically and order any repeated excerpts based on their appearance.

Ajami et al. (2017):AWAP potential evapotranspiration is calculated based on the Priestley–Taylor equation (Raupach et al., 2009). **Anabalón and Sharma (2017):** For most of the datasets, the correlations in water–limited environments were higher between AET and PP. In energy-limited regions, the results were mixed: MOD16, GLEAM v3a, E2O-ORCH, and E2O-PG presented higher correlations between AET and PET trends, while in the remaining datasets, the correlations were higher between AET and PP trends.

Anabalón and Sharma (2017): To compare the directions and statistical significance of the trends found in the different datasets, theDataConcurrenceIndex(DCI),introducedbyAnabalón [2016] was used. This index compares the total number of positive significant trends versus the total number of negative significant trends, as expressed below. where ND is the number of databases with information, STi is the magnitude of the trend, and hi is a binary variable that indicate if there is a significant trend (1) or not (0) for database i.TheDCIiscalculatedonevery cell with information, therefore it allows one to assess the spatial distribution of the differences in the trends.

Anabalón and Sharma (2017): Figure 1d shows a completely different picture of the multidecadal PET trends when compared with those derived for the short-term period. Most of the world exhibits mid to high concurrence of increasing PET, particularly Europe, South America, and Northern Africa. The regions under null DCI are reduced considerably, and the negative DCI

zones are concentrated in a few regions in the tropical range. Table 4 shows the land surface coverage of the long-term PET DCI.

Anabalón and Sharma (2017): For most of the datasets, the correlations in water–limited environments were higher between AET and PP. In energy-limited regions, the results were mixed: MOD16, GLEAM v3a, E2O-ORCH, and E2O-PG presented higher correlations between AET and PET trends, while in the remaining datasets, the correlations were higher between AET and PP trends.

Aouissi et al. (2016): The methods integrated in SWAT to estimate PET (PM, HA, PT) had little influence on monthly streamflow and actual ET predictions, because runoff is well induced by precipitation and the period of high ET does not correspond to the wet season.

Bai et al. (2016): In runoff modeling, different PET inputs can produce similar runoff simulations in both nonhumid and humid regions. However, when estimating AET and WSC in humid regions, different PET inputs will result in significantly different AET and WSC simulations, which should be noted by model users.

Bai et al. (2016): The reasons for the insensitivities of runoff simulations to PET inputs are attributed to model parameter calibration, which is able to eliminate the discrepancies in model inputs and generate similar runoff simulation results.

Bai et al. (2016): Different PET inputs mainly affect AET and WSC in humid regions, and the sums of WSC and AET values are similar across different PET drivers in humid regions, as are the runoff values.

Bai et al. (2016): The water balance components in nonhumid regions are mainly controlled by precipitation rather than PET, resulting in a good agreement between water balance components, even though the PET inputs are considerably different.

Berghuijs et al. (2017): The absolute elasticity of runoff to potential evaporation changes is always lower than the elasticity to precipitation changes. The global pattern indicates that for 83% of the land grid cells runoff is most sensitive to precipitation changes, while other factors dominate for the remaining 17%. This dominant role of precipitation contradicts previous global assessments, which considered the impacts of aridity changes as a ratio.

Birhanu et al. (2018): The hydrological models' performance was satisfactory for each PET input in the calibration and validation periods for all of the tested catchments. The five hydrological models' performance were found to be insensitive to the 12 PET inputs because of the SCE-UA algorithm's efficiency in optimizing model parameters. However, the five hydrological models' parameters in charge of transforming the PET to actual evapotranspiration were sensitive and significantly affected by the PET complexity.

Boeing et al. (2024): Figure 3. (A) yearly TWS anomalies 1766–2022, colored bars denote the length of the recovery periods. (B) and (C) depict yearly P and E flux anomalies. The thick line in all subplots is a 30 year running mean to depict long–term trends. The points denote significant positive or negative 30-year trends including the year where the point is marked and 29 preceding years. The mean climatology for the anomalies in (A)–(C) is calculated based on the 1766–2022 period. Note that the y-axes have different limits to enhance the visibility.

Bruno and Duethmann (2024): Variations in EC wererelated with variations in precipitation and radiation, with a potentially increasing influence of precipitationafter 2000s.

Devia et al. (2015): In general, rainfall-runoff models are the standard tools used for investigating hydrological processes. A

large number of models with different applications ranges from small catchments to global models has been developed. Each model has got its own unique characteristics and respective applications. Some of them are comprehensive and uses the physics of underlying hydrological processes and are distributed in space and time.

Guo et al. (2017): The two PET models consistently indicated temperature to be the most important variable for PET, but showed large differences in the relative importance of the remaining climate variables. In particular for the Penman–Monteith model, wind and relative humidity were the second-most important variables for dry and humid catchments, respectively, whereas for the PriestleyTaylor model solar radiation was the second-most important variable, with the greatest influence in warmer catchments. This information can be useful to inform the selection of suitable PET models to estimate future PET for different climate conditions, providing evidence on both the structural plausibility and input uncertainty for the alternative models.

Hanselmann et al. (2024): Jensen-Haise estimates a relatively stable high PET from mid-June to the end of July, with the highest values of 1.3 mm/day in mid-July.

Hua et al. (2020): For the entire arid zone, the PM method overestimated the potential evapotranspiration by 33.7 mm per year, with an overestimation of 29.0 mm from July to August. The most significant overestimation was evident in the mountainous and plain nonvegetation areas, in which the annual mean overestimation reached 5% and 10%, respectively; during July, there was an estimation of 10% and 20%, respectively. Although the annual evapotranspiration of the plains with better vegetation coverage was slightly underestimated, overestimation still occurred in July and August, with a mean overestimation of approximately 5%.

Jung et al. (2013): Runoff sensitivity can readily explain the conflicting directions of AET changes under similar precipitation change. Under increasing precipitation, AET decreases when runoff is increasing more rapidly than precipitation based on the water balance. Conversely, AET increases when runoff is decreasing more rapidly than precipitation.

Kuentz et al. (2017): Table 1. Catchment descriptors and the original source of information. Type of descriptor is indicated in brackets after variable name (T: topography; LC: land cover; S: soil type; G: geology; C: climate). Variables marked with grey color were removed from the analysis because no significant correlation was found between these and the flow signatures (see Sect. 2.3).

Liu et al. (2022): ETp and ETa in most parts of the world indicated an increasing trend ($Z > 0$), but the spatial distribution of the increasing trend of the two was quite different. ETp had a remarkable increasing trend in the Ural Mountains on the border between Asia and Europe, the Appalachian Mountains and Mount Whitney in North America (α=0.05, $Z > 1.96$) (Fig. 4d), while ETa in these areas did not show an increasing trend but even declined (Fig. 4e). ETa had a marked increasing trend in the Amazon Plain, Congo Basin, South Asia and East Asia. Since water storage changes (TWC and NWC) are water losses caused by evapotranspiration, there is a strong negative correlation with ETp, ETa and Er, but the human water changes (HWC) are positively correlated, notably in Peru, Congo, Brasilia, and Indonesia (Fig. S6e in supplementary information) where the large-scale irrigation system and irrigation water accelerate ETa

Lu et al. (2005): The commonly used PET methods for this comparison study gave a wide range of values, showing differences in PET across the southeastern United States among six methods as high as 500 mm/yr.

Maček et al. (2018): Table 3. Slope (k) of the linear regression for the radiative and aerodynamics components of the ET0 and average relative contribution of radiative and aerodynamics components to the total ET0.

Massari et al. (2022): he climate of the specific basin was defined based on the aridity index, which we calculated as the ratio between long-term average annual potential evaporation and precipitation (both from ERA5) (Unesco, 1979).

Massari et al. (2022): We relied on multidecadal records of streamflow and precipitation for more than 200 catchment areas across various European climates, which distinctively show the emergence of similar periods of exacerbated runoff deficit identified in previous studies, i.e. runoff deficit on the order of -20 % to -40 % less than what expected from precipitation deficits. The magnitude of this exacerbation is two to three times larger for basins located in dry regions than for basins in wet regions, and is qualitatively correlated with an increase in annual evaporation during droughts, in the order of +11 % and +33 % over basins characterized by energy-limited and water-limited evaporation regimes, respectively. Thus, enhanced atmospheric and vegetation demand for moisture during dry periods induces a nonlinear precipitation-runoff relationship for low-flow regimes, which results in an unexpectedly large decrease in runoff during periods of already low water availability.

Massari et al. (2022): Runoff exacerbation is related to an increase in evaporation occurring under two defined and concurrent preconditions: (1) water storage can support ET during the drought period, and (2) there is a sufficient vapour-pressure deficit (mainly driven by the temperature increase) to generate evaporation.

Mazzoleni et al. (2019): Precipitation datasets belonging to Class 2 outperformed the other datasets in basins with Tropical and Temperate-Arid climate (e.g. Congo, Mississippi and Godavari), while Class 3 datasets showed the highest NSE values in Temperate and Temperate-Cold basins (e.g. Danube, Rhine and Volga). In addition, datasets from Class 3 gave the best performances at basin outlets in case of dense precipitation monitoring networks, as in the Danube and Rhine basins.

Ndiaye et al. (2024): Observed and reanalysis data are used to calculate daily PET values according to 21 methods. Combinatory methods and temperature-based methods provide the most accurate estimation. However, the aerodynamic methods underestimate PET and some temperature and radiation-based methods (Heydari and Heydari and Priestley-Taylor) overestimate it. With regard to the sensitivity of GR models to the different PET estimation methods, all three GR models showed an ability to readjust the estimation errors of the PET methods.

Oudin et al. (2005): The second step confirmed that the four rainfallrunoff models considered here do not significantly benefit from PE. This is quite disconcerting from a modelling point of view, because a better streamflow simulation is expected when using a more relevant evaporative demand. Rainfall-runoff models are poorly responsive to observed classical Penman PE

Oudin et al. (2005): The first step of our study consisted in confirming this suspicion over a large and climatically varied catchment sample, as well as for several representative rainfall-runoff models. The conclusion is that looking for daily observed PE data as inputs into a rainfall-runoff model is not necessary: a long-term average regime curve will serve as well. One of the purposes of this article was to generalize previous results found in the literature and our conclusions substantiate these findings.

Pfeifroth et al. (2018): Box plot of the regional trends (W/m2/decade) of surface solar radiation at the station locations (white) based on stations, (red) SARAH-2, and (blue) CLARA-A2 data, including mean trends (diamonds). Outliers are shown as dots. Regions: CE = central east, CW = central west, NW = northwest, S = south, and N = north. For each region the plot area is

divided into trends for the full time period 1983–2015 (for stations and SARAH-2) and trends for the time period 1992–2015 (for stations, SARAH-2, and CLARA-A2).

Pimentel et al. (2023): Figure 2. Global distribution of best PET formula according to: (a) MOD16 PET (115,151 catchments), (b) MOD16 AET (115,151 catchments), and (c) streamflow observations (4,367 catchments).

Pimentel et al. (2023): Hargreaves was the best PET formula in 50% of the catchments, most of them located in the Amazonas, central Europe, and Oceania; Jensen-Haise was better for catchments in northern latitudes (36%). Finally, Priestley-Taylor was the best formula for India and latitudes above 65° North.

Pimentel et al. (2023): nally, the assessment against independent streamflow gauges shows a clear predominance of Priestley-Taylor as the best formula to use as a compromise world-wide (Figure 3c), as it minimizes the RE in about 56% of the analyzed catchments (Table 3, column 7). Jensen-Haise is a suitable alternative PET formula in central North America, South Africa and some spots in central Europe, central Asia, and Australia.

Reaver et al. (2022): The Budyko framework posits that a catchment's long-term mean evapotranspiration (ET) is primarily governed by the availabilities of water and energy, represented by long-term mean precipitation (P) and potential evapotranspiration (PET), respectively.

Seiller and Anctil (2016): The choice of the PET formula moderately affected the calibration efficiency, except for some formulas leading to much larger PET quantities than others, but hydrological models, during their calibration process, adapted their parameters so that efficiency was maximized.

Shi et al. (2023): In specific, JH produced excellent or good estimation of annual ETp across all stations and Tu produced good or fair estimation of annual ETp across all stations.

Teuling et al. (2019): In much of central-western Europe, our results show an increase in evapotranspiration of the order of 5 %–15 % between 1955–1965 and 2005–2015, whereas much of the Scandinavian peninsula shows increases exceeding 15 %. The Iberian Peninsula and other parts of the Mediterranean show a decrease of the order of 5 %–15 %. A similar north–south gradient was found for changes in streamflow, although changes in central-western Europe were generally small. Strong decreases and increases exceeding 45 % were found in parts of the Iberian and Scandinavian peninsulas, respectively. In Sweden, for example, increased precipitation is a larger driver than large-scale reforestation and afforestation, leading to increases in both streamflow and evapotranspiration. In most of the Mediterranean, decreased precipitation combines with increased forest cover and potential evapotranspiration to reduce streamflow. In spite of considerable local- and regional-scale complexity, the response of net actual evapotranspiration to changes in land use, precipitation, and potential evaporation is remarkably uniform across Europe, increasing by $\sim$ 35–60 km3 yr-1, equivalent to the discharge of a large river. For streamflow, effects of changes in precipitation ($\sim$ 95 km3 yr-1) dominate land use and potential evapotranspiration contributions ($\sim$ 45–60 km3 yr-1).

Thornthwaite (1948): The vegetation of the desert is sparse and uses little water because water is deficient. If more water were available, the vegetation would be less sparse and would use more water. There is a distinction, then, between the amount of water that actually transpires and evaporates and that which would transpire and evaporate if it were available. When water supply increases, as in a desert irrigation project, evapotranspiration rises to a maximum that depends only on the climate. This we may call "potential evapotranspiration," asdistinct from actual evapotranspiration

Voisin et al. (2008): Globally and in every continent, simulated runoff is much more sensitive to precipitation differences than evapotranspiration.

Wang et al. (2023): First, the hydrological model can often adapt to some inaccurate rainfall inputs showing good streamflow simulation to some extent. The overall rainfall BIAS helps in predicting hydrological model adaptability to rainfall data sets. Furthermore, the hydrological model adaptability has an adaptable threshold of overall rainfall BIAS, which is -140 mm for our study (total rainfall is about 518 mm). Second, hydrological model adaptability is not only affected by the overall rainfall BIAS but also significantly influenced by the event-based rainfall BIAS. How the event-based rainfall bias of rainstorms shapes the overall rainfall bias affects hydrological model adaptability. In particular, the rainfall accuracy during the heaviest rainstorm which results in peak flow has a large impact. The hydrological model would be unable to adapt well to the large overall rainfall bias that is mainly caused by a significant underestimation of the severest rainstorm.

Xiang et al. (2020): Early applications of ETp were in meteorology and hydrology, but later its applications were extended to other fields (Parajuli et al., 2019; Zhang et al.,2019a,b). For example, in agronomy it was related to crop water requirements and irrigation scheduling (Yao et al., 2020; Feng et al., 2019).

Zhang et al. (2016): The dominant contributor to ET variability is ET0 under energy-limited condition (aridity index $\leqslant 0.76$), whereas the dominant contributor is precipitation under equitant ($0.76 <$ aridity index $\leqslant 1.35$) and water-limited conditions (aridity index $\geqslant 1.35$). The contribution of ET0 to ET variability decreases with the aridity index, whereas the contribution of precipitation to ET variability increases with the aridity index.

Zhang et al. (2016): Fig. 2. The long-term hydroclimatological characteristics of the 282 catchments based on Budyko hypothesis. All the catchments are classified into three climate conditions: energy-limited condition (where aridity index (ET0/P) $\leqslant 0.76$), equitant condition ($0.76 <$ aridity index $\leqslant 1.35$) and water-limited condition (aridity index $\geqslant 1.35$).

Zhang et al. (2016): ET0 is estimated by the Penman formula (Penman, 1948, Shuttleworth, 1993), which is showed to be the most appropriate form when considering a changing climate (Donohue et al., 2010a, McVicar et al., 2012a). **Zhao et al. (2013):** There are two groups of evapotranspiration estimation methods in hydrological models: one first estimates separately water surface evaporation, soil evaporation and vegetable transpiration, and then integrates them to get the basin evapotranspiration depending on the land use pattern. The other one first estimates potential evapotranspiration (ETp) and then converts it into actual evapotranspiration (ETa) applying the Soil Moisture Extraction Function. In this paper the first type methods are called the classification gathering methods, while the second – the integrated converting methods.

Text S2. Seasonal changes in hydrological cycle components

The summer season (DJF) exhibits the smallest changes across each hydrological component (Figure S1). For PET, temperature-based methods indicate a strong positive trend compared to combination-type methods in energy-limited and mixed catchments. Blaney-Criddle demonstrates the largest trend among all methods for energy-limited and mixed catchments, while Hargreaves-Samani presents the largest trend in water-limited catchments. Only the Thornthwaite method indicates a negative trend for water-limited catchments. For AET, the trend patterns for each PET method are similar to those observed for PET. In energy-limited and mixed catchments, temperature-based and energy-based methods reflect positive changes at the median level, while combination-type methods indicate no change in AET. In water-limited catchments, combination-type methods present the most pronounced changes, around 0.1 mm seas^{-1} year^{-1}, whereas Thornthwaite indicates a negative trend (Figure S1). Almost all PET methods indicate similar changes in Q across catchment categories. For TWS, energy-limited catchments appear insensitive to the PET method selection, while in mixed catchments, all PET methods show negative changes, with Hargreaves-Samani demonstrating the most negative trend and Blaney-Criddle reflecting the greatest variability. In water-limited catchments, all PET methods indicate negative changes except for Blaney-Criddle and the Milly-Dunne method.

In the spring season (MAM), all PET methods demonstrate positive changes in PET for each catchment category (Figure S2). The Hargreaves-Samani method exhibits the highest trend, followed by Blaney-Criddle, across all catchment types for PET. The overall variability in PET methods decreases from energy-limited to mixed, and then to water-limited catchments. For AET (Figure S2), all PET methods reflect a positive trend in each catchment category. In energy-limited and mixed catchments, Blaney-Criddle and Hargreaves-Samani reveal the highest trends, with Hargreaves-Samani leading in energy-limited catchments. Radiation and combination-type methods demonstrate greater variability compared to temperature-based methods in energy-limited catchments, while in mixed catchments, temperature-based methods reveal greater variability. In water-limited catchments, the Blaney-Criddle method exhibits larger variability. Q indicates almost no change among PET methods in energy-limited catchments (Figure S2). However, in water-limited catchments, Blaney-Criddle indicates the least change, while other PET methods exhibit approximately 0.5 mm seas^{-1} year^{-1}. In water-limited catchments, Blaney-Criddle reflects the least change, while the highest trend (0.4 mm seas^{-1} year^{-1}) is indicated by the Thornthwaite method. Overall, energy-limited methods reflect higher trends compared to temperature and combination-type methods. TWS remains largely insensitive to PET method selection for energy-limited catchments. For mixed catchments, Hargreaves-Samani demonstrates the highest negative trend compared to the median of other PET methods (Figure S2). For water-limited catchments, all PET methods demonstrate positive trends for the TWS hydrological component. The variability of energy and combination-type methods is less than that of temperature-based methods in mixed catchment categories. Among the temperature-based methods, Blaney-Criddle exhibits higher variability in mixed and water-limited catchments. In water-limited catchments, Blaney-Criddle shows the highest positive trend, followed by the energy-based Milley and Dunne method.

In the autumn season (SON), all PET methods reflect trends similar to those in the summer season, but with reduced magnitudes (Figure S3). The Jensen-Haise method records the highest trends, with median values of approximately 0.2, 0.3, and 0.5 mm seas^{-1} year^{-1} for energy-limited, mixed, and water-limited catchments, respectively. For AET, all PET methods

indicate a positive trend compared to the median. water-limited catchments exhibit greater variability in response to PET methods than energy-limited and mixed catchments. In mixed catchments, nearly zero trends are observed across all PET methods, with Blaney-Criddle and Jensen-Haise demonstrating higher variability. Q shows little sensitivity to trends in PET method across all catchment categories, with slight variability observed among the methods within each catchment category. For TWS, energy-limited and mixed catchments are largely unaffected to the PET method selection, except for Jensen-Haise, which shows a negative trend. Although there is slight variation among PET methods within each category, mixed behavior is observed in water-limited catchments. Some temperature-based methods, such as Blaney-Criddle, McGuinness-Bordne, and Hargreaves-Samani, indicate positive trends, while others reflect negative trends. All combination-type methods, like Penman-Monteith and modified Penman-Monteith[CO_2], demonstrate negative trends.

Table S1. Table represents the number of catchments in each category under different scenarios. For instance, the "All" column represents the inclusion of all PET methods for catchment classification, the "MB" column represents all methods except MB, and the "MB-BC" column includes all PET methods except for MB and BC.

Category	All	JH	BC	TH	MB–BC	BC–JH	MB–JH	MB–JH–BC
Energy-Limited	189	197	235	189	235	306	197	417
Mixed	330	322	284	325	284	213	322	102
Water-Limited	34	34	34	39	34	34	34	34

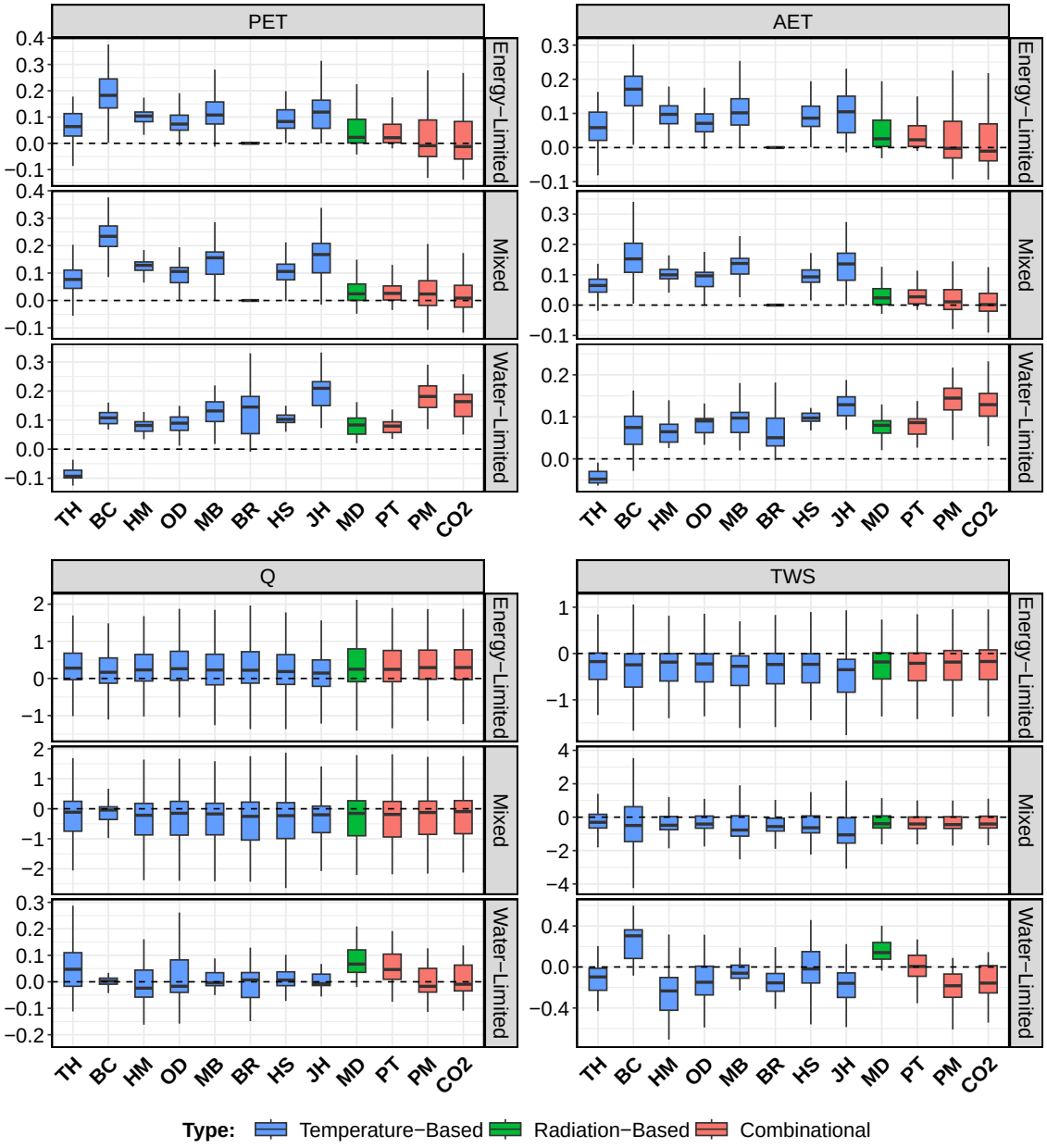

Figure S1. Boxplot represents the seasonal (summer season (DJF)) trends of different PET methods for AET, and Q across three categories of catchment: energy-limited, mixed, and water-limited. The whiskers represent the 10th and 90th percentiles, and the box encompasses the 25th and 75th percentiles, with the median represented by the black line within the box. Trend units are in mm seas^{-1} year^{-1}.

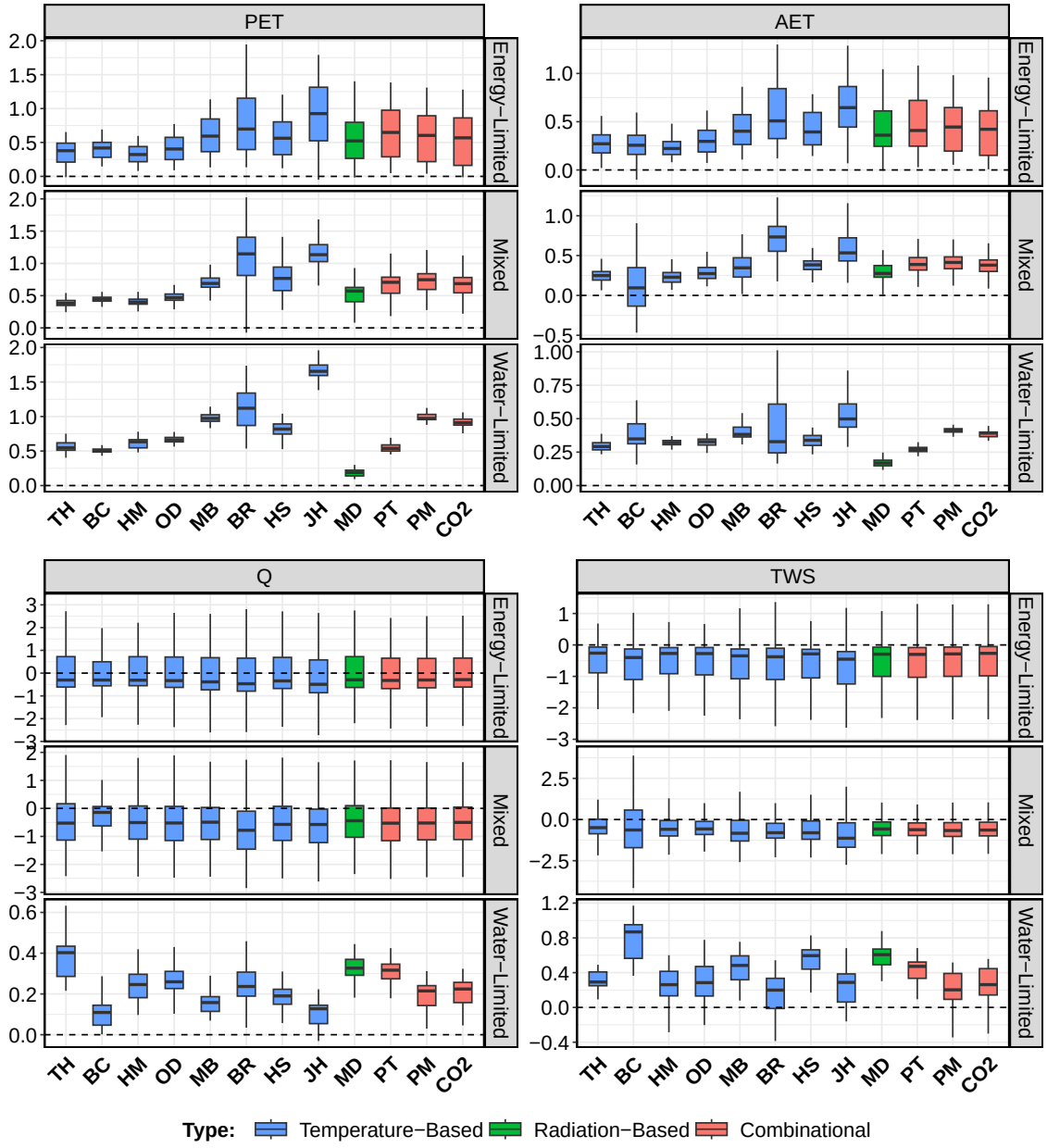

Figure S2. Boxplot represents the seasonal (spring season (MAM)) trends of different PET methods for AET, and Q across three categories of catchment: energy-limited, mixed, and water-limited. The whiskers represent the 10th and 90th percentiles, and the box encompasses the 25th and 75th percentiles, with the median represented by the black line within the box. Trend units are in mm seas^{-1} year^{-1}.

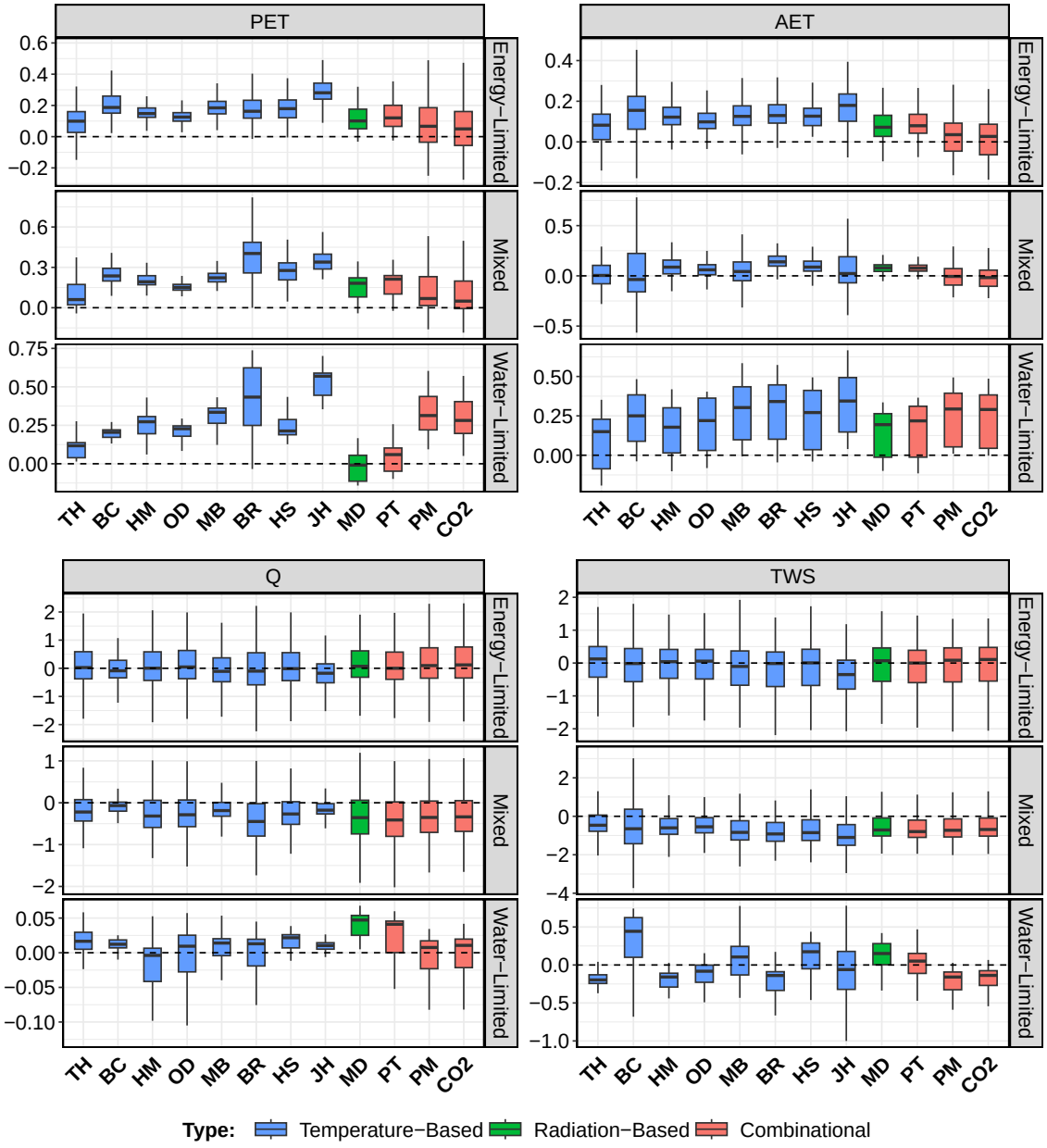

Figure S3. Boxplot represents the seasonal (autumn season (SON)) trends of different PET methods for AET, and Q across three categories of catchment: energy-limited, mixed, and water-limited. The whiskers represent the 10th and 90th percentiles, and the box encompasses the 25th and 75th percentiles, with the median represented by the black line within the box. Trend units are in mm seas^{-1} year^{-1}.

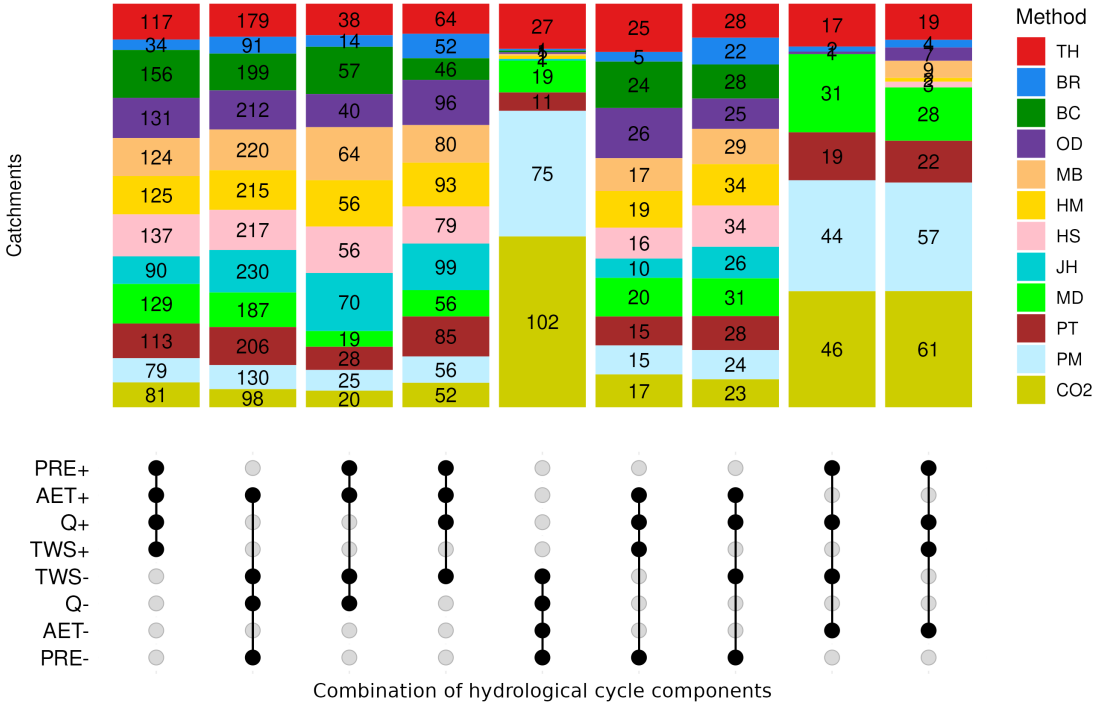

Figure S4. The figure shows the combination of trends for different hydrological components and the corresponding influence of PET methods for the summer season (DJF). PRE+, AET+, Q+, and TWS+ represent the positive trends for precipitation, AET, Q, and TWS respectively. Similarly, pre-, AET-, Q- and TWS- represent negative trends. Where PRE is precipitation, AET is actual evapotranspiration, Q is runoff and TWS is total water storage. Abbreviations used for different PET methods are TH: Thornthwaite, BR: Bair-Robertson, BC: Blaney-Criddle, OD: Oudin, MB: McGuinness-Borden, HM: Hamon, HS: Hargreaves-Samani, JH: Jensen-Haise, MD: Milly-Dunne, PT: Priestley-Taylor, PM: Penman-Monteith, CO_2: Modified Penman-Monteith accounts CO_2.

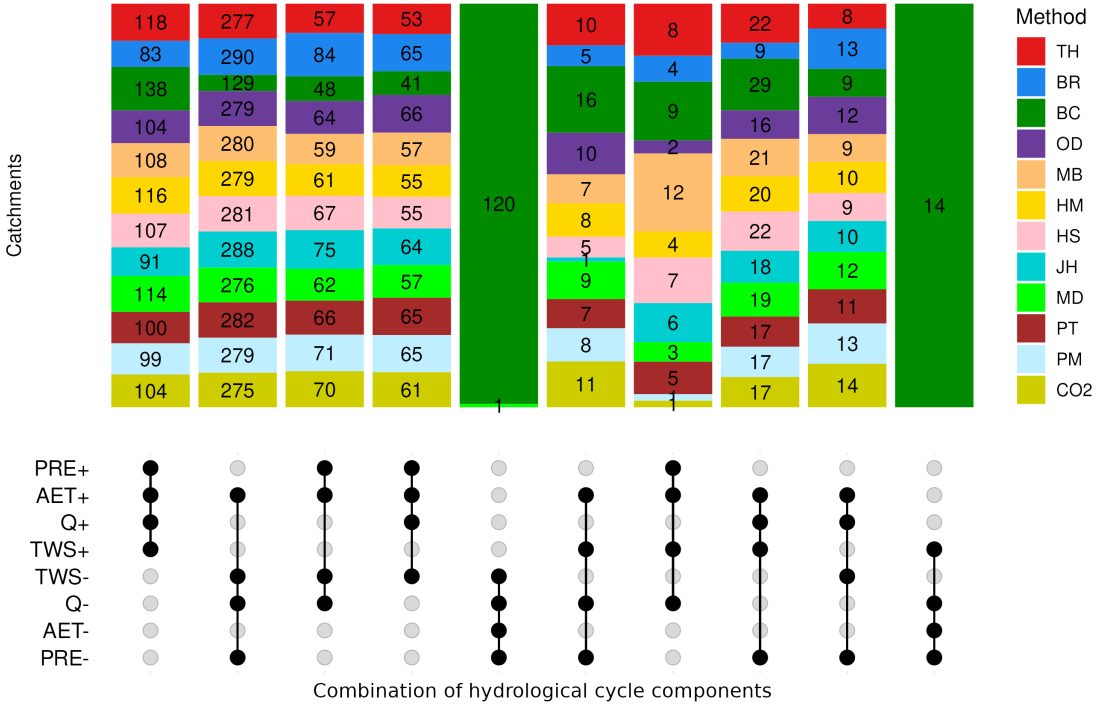

Figure S5. The figure shows the combination of trends for different hydrological components and the corresponding influence of PET methods for the spring season (MAM). PRE+, AET+, Q+, and TWS+ represent the positive trends for precipitation, AET, Q, and TWS respectively. Similarly, PRE-, AET-, Q-, and TWS- represent negative trends. Where PRE is precipitation, AET is actual evapotranspiration, Q is runoff and TWS is total water storage. Abbreviations used for different PET methods are TH: Thornthwaite, BR: Bair-Robertson, BC: Blaney-Criddle, OD: Oudin, MB: McGuinness-Borden, HM: Hamon, HS: Hargreaves-Samani, JH: Jensen-Haise, MD: Milly-Dunne, PT: Priestley-Taylor, PM: Penman-Monteith, CO_2: Modified Penman-Monteith accounts CO_2.

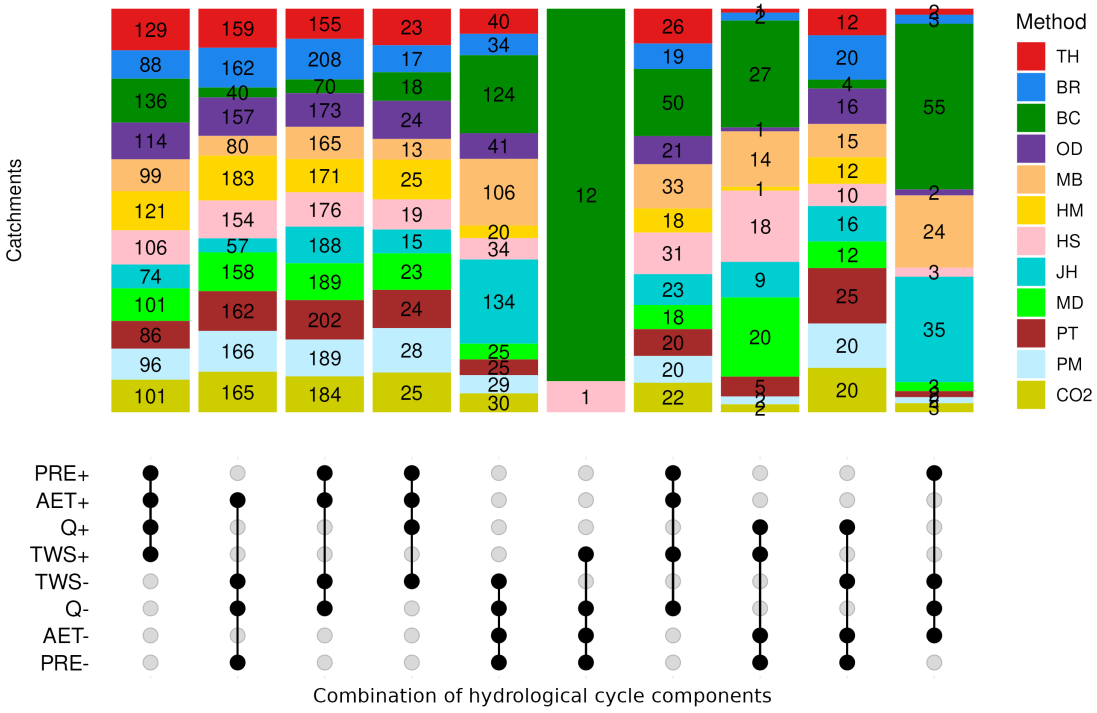

Figure S6. The figure shows the combination of trends for different hydrological components and the corresponding influence of PET methods for the summer season (JJA). PRE+, AET+, Q+, and TWS+ represent the positive trends for precipitation, AET, Q, and TWS respectively. Similarly, PRE-, AET-, Q-, and TWS- represent negative trends. Where PRE is precipitation, AET is actual evapotranspiration, Q is runoff and TWS is total water storage. Abbreviations used for different PET methods are TH: Thornthwaite, BR: Bair-Robertson, BC: Blaney-Criddle, OD: Oudin, MB: McGuinness-Borden, HM: Hamon, HS: Hargreaves-Samani, JH: Jensen-Haise, MD: Milly-Dunne, PT: Priestley-Taylor, PM: Penman-Monteith, CO_2: Modified Penman-Monteith accounts CO_2.

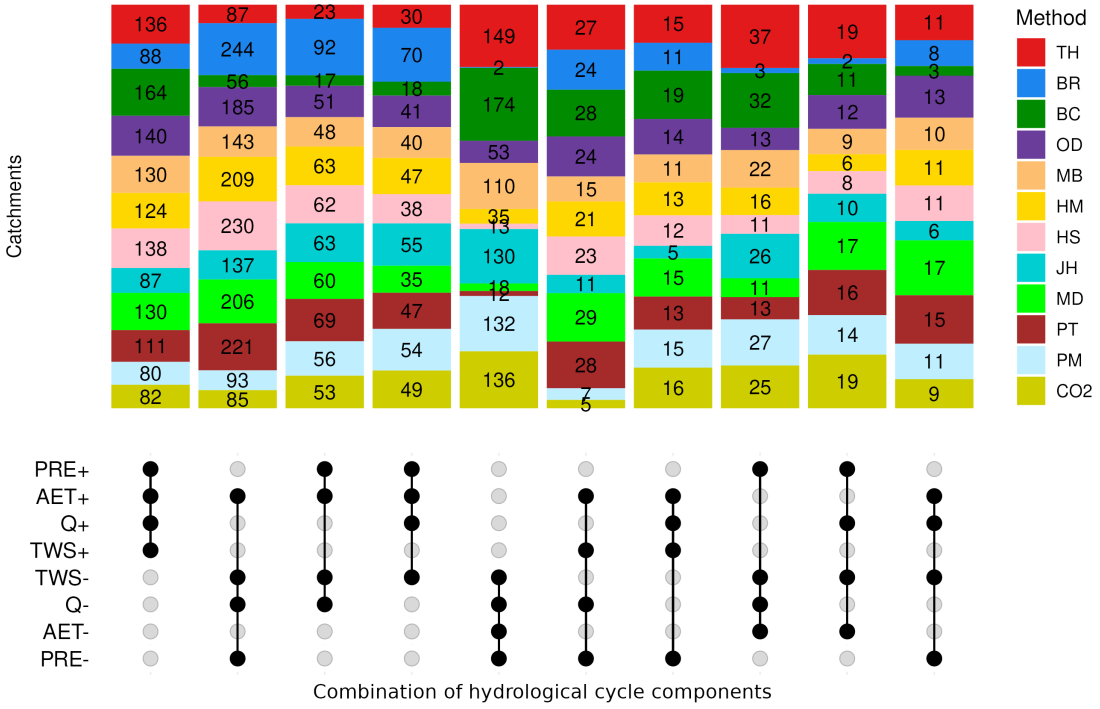

Figure S7. The figure shows the combination of trends for different hydrological components and the corresponding influence of PET methods for the autumn season (SON). PRE+, AET+, Q+, and TWS+ represent the positive trends for precipitation, AET, Q, and TWS respectively. Similarly, PRE-, AET-, Q-, and TWS- represent negative trends. Where PRE is precipitation, AET is actual evapotranspiration, Q is runoff and TWS is total water storage. Abbreviations used for different PET methods are TH: Thornthwaite, BR: Bair-Robertson, BC: Blaney-Criddle, OD: Oudin, MB: McGuinness-Borden, HM: Hamon, HS: Hargreaves-Samani, JH: Jensen-Haise, MD: Milly-Dunne, PT: Priestley-Taylor, PM: Penman-Monteith, CO_2: Modified Penman-Monteith accounts CO_2.

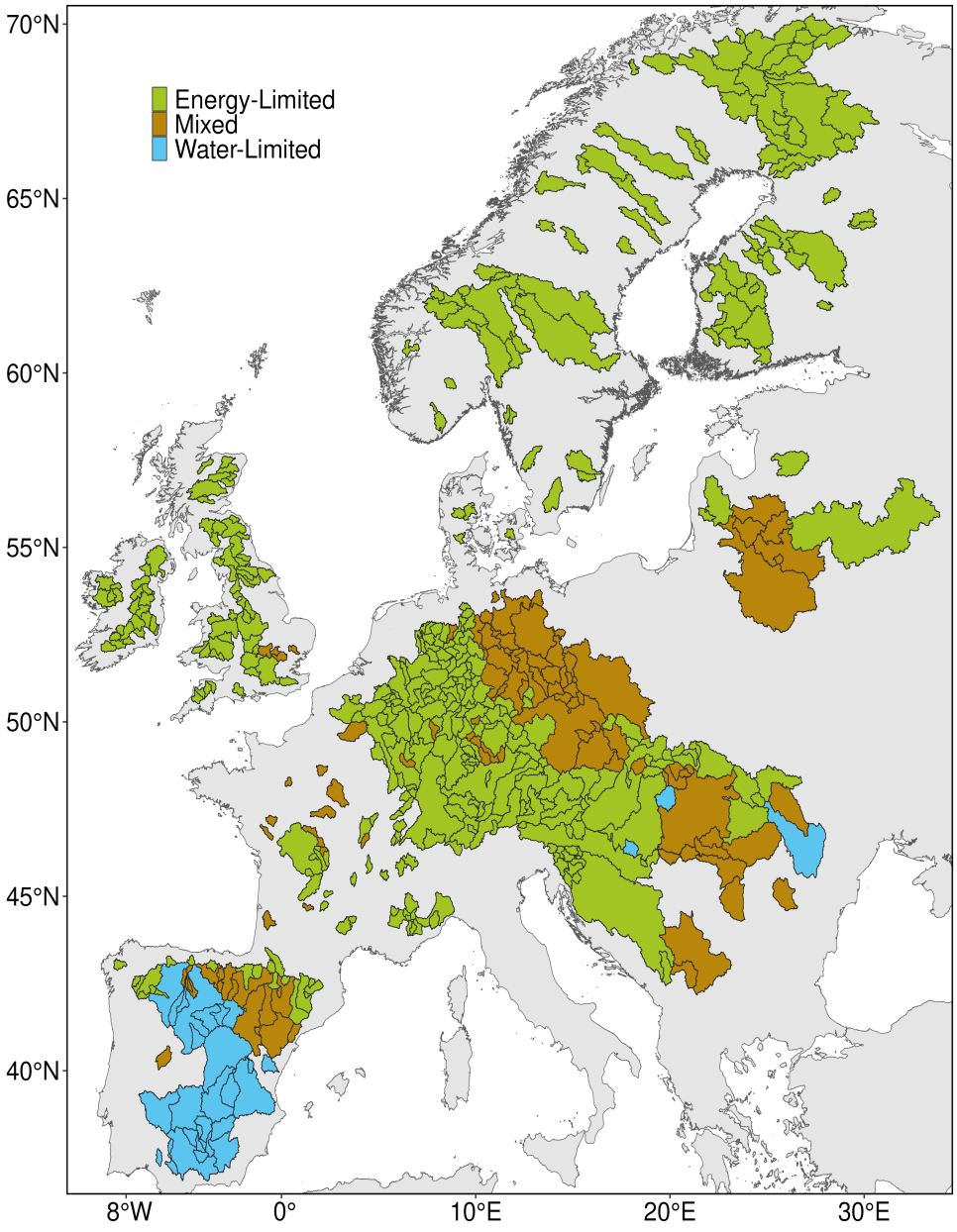

Figure S8. Catchment classification by excluding three PET methods namely Jensen-Haise, McGuinness-Bordne and Blaney-Criddle

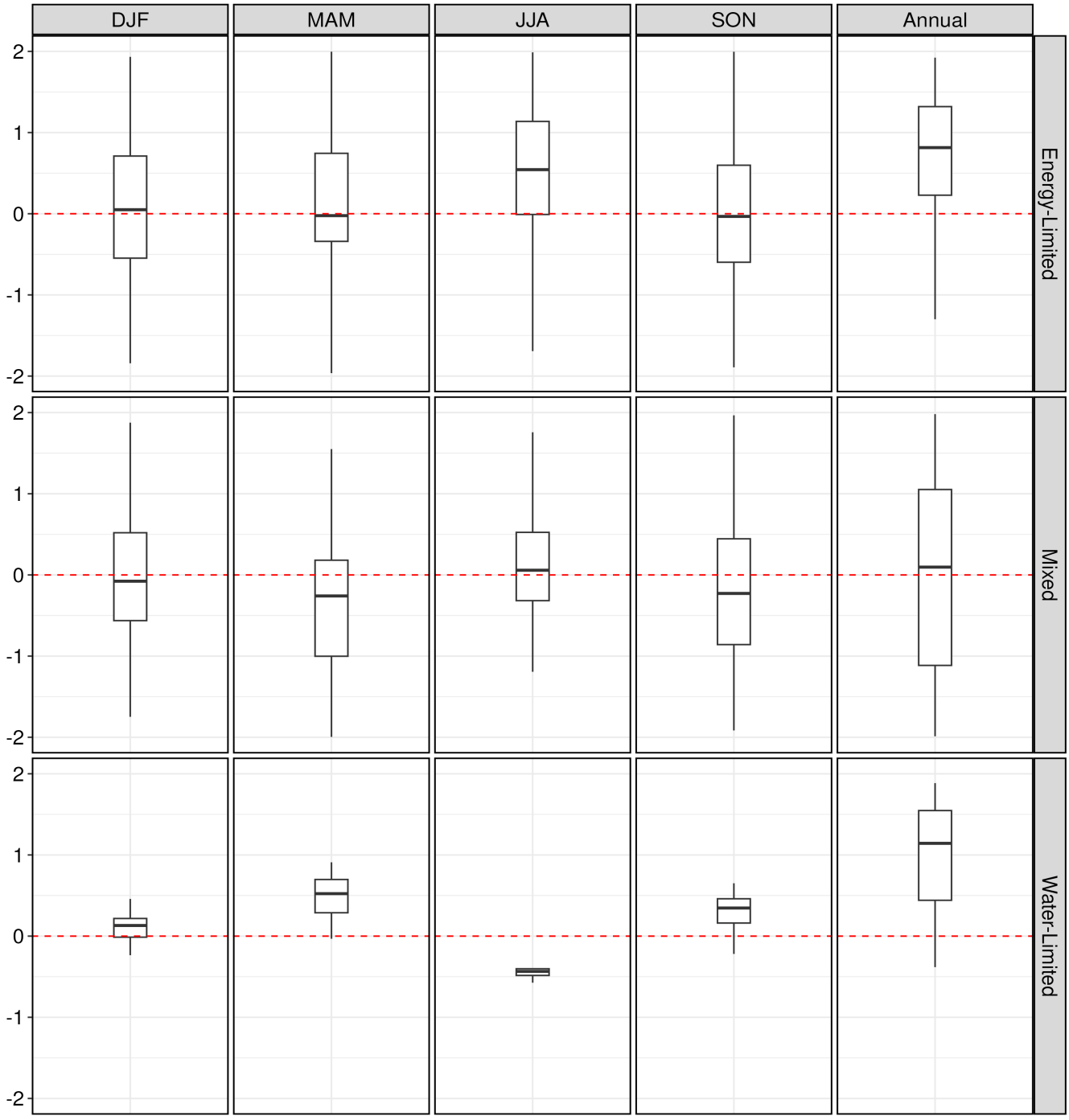

Figure S9. Seasonal and annual precipitation trend, with annual units in mm/year and seasonal units in mm seas^{-1} year^{-1}.

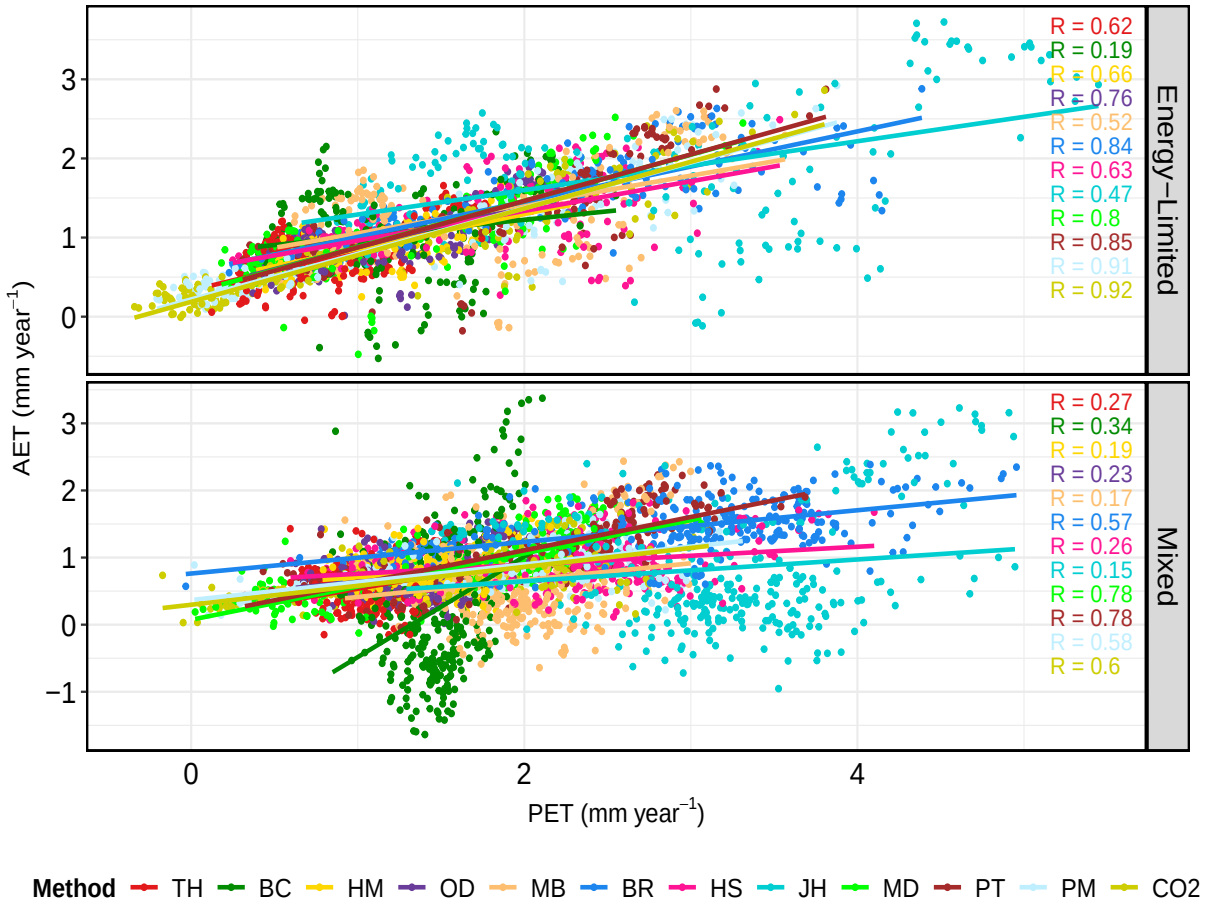

Figure S10. Correlation between trends of AET and PET for energy-limited and mixed catchments catchment category corresponding to each PET method. Abbreviations used for hydrological cycle components are as follows: PET, AET, Q and, TWS represent potential evapotranspiration, actual evapotranspiration, runoff and, total water storage, respectively. Abbreviations used for different PET methods are TH: Thornthwaite, BR: Bair-Robertson, BC: Blaney-Criddle, OD: Oudin, MB: McGuinness-Borden, HM: Hamon, HS: Hargreaves-Samani, JH: Jensen-Haise, MD: Milly-Dunne, PT: Priestley-Taylor, PM: Penman-Monteith, CO_2: Modified Penman-Monteith accounts CO_2.

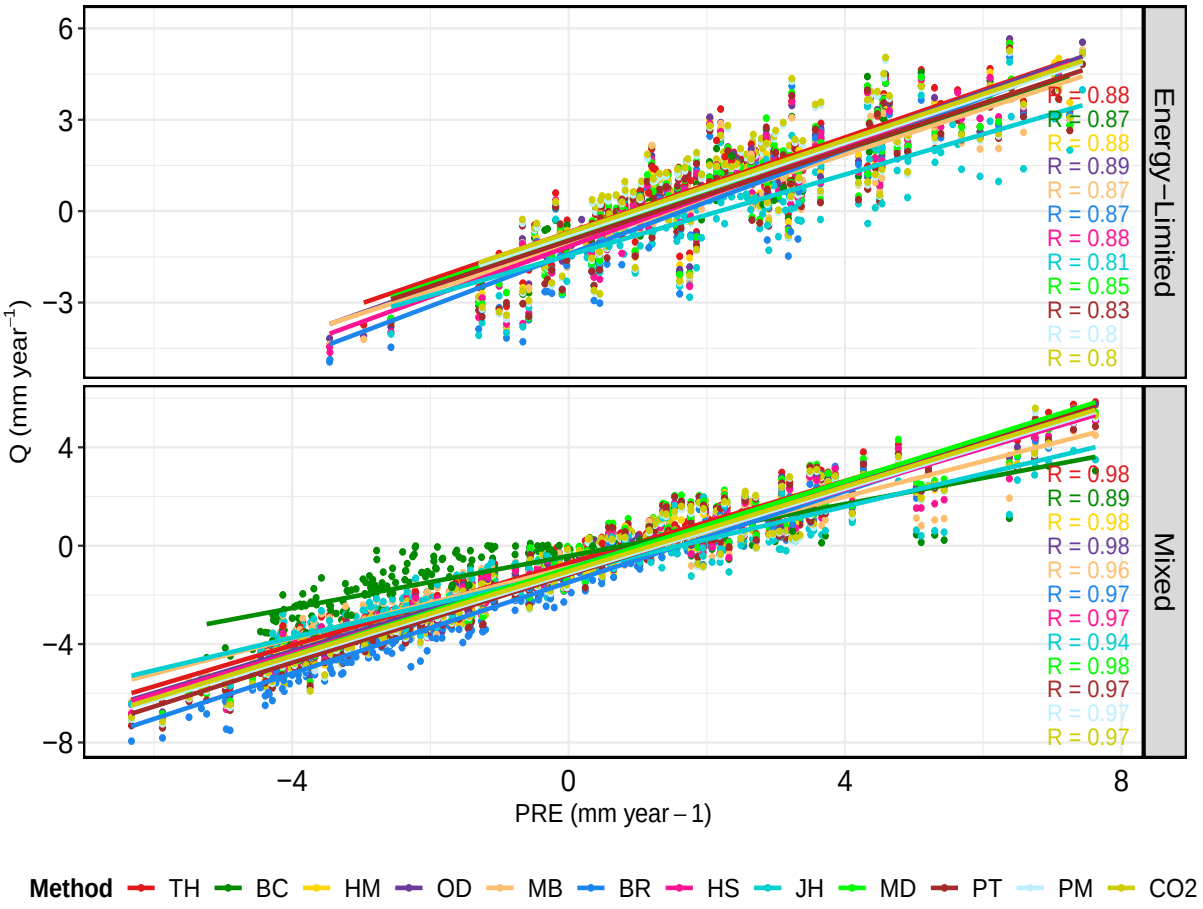

Figure S11. Correlation between trends of Q and PRE for energy-limited and mixed catchments catchment category corresponding to each PET method. Abbreviations used for hydrological cycle components are as follows: PET, AET, Q, TWS, and PRE represent potential evapotranspiration, actual evapotranspiration, runoff, total water storage, and precipitation, respectively. Abbreviations used for different PET methods are TH: Thornthwaite, BR: Bair-Robertson, BC: Blaney-Criddle, OD: Oudin, MB: McGuinness-Borden, HM: Hamon, HS: Hargreaves-Samani, JH: Jensen-Haise, MD: Milly-Dunne, PT: Priestley-Taylor, PM: Penman-Monteith, CO_2: Modified Penman-Monteith accounts CO_2.

Figure S12. Seasonal trend contribution in annual trend for each catchment category for PET and all the hydrological components (AET, Q, and TWS). Abbreviations used for hydrological cycle components are as follows: PET, AET, Q and, TWS represent potential evapotranspiration, actual evapotranspiration, runoff and, total water storage, respectively. Abbreviations used for different PET methods are TH: Thornthwaite, BR: Bair-Robertson, BC: Blaney-Criddle, OD: Oudin, MB: McGuinness-Borden, HM: Hamon, HS: Hargreaves-Samani, JH: Jensen-Haise, MD: Milly-Dunne, PT: Priestley-Taylor, PM: Penman-Monteith, CO_2: Modified Penman-Monteith accounts CO_2. For seasons DJF, MAM, JJA, and SON indicate summer, spring, summer, and autumn, respectively. Y-axis units are in mm/seas/year.

References

Ajami, H., Sharma, A., Band, L. E., Evans, J. P., Tuteja, N. K., Amirthanathan, G. E., and Bari, M. A.: On the non-stationarity of hydrological response in anthropogenically unaffected catchments: an Australian perspective, Hydrology and Earth System Sciences, 21, 281–294, https://doi.org/10.5194/hess-21-281-2017, 2017.

Anabalón, A. and Sharma, A.: On the divergence of potential and actual evapotranspiration trends: An assessment across alternate global datasets, Earth's Future, 5, 905–917, https://doi.org/10.1002/2016EF000499, 2017.

Aouissi, J., Benabdallah, S., Lili Chabaâne, Z., and Cudennec, C.: Evaluation of potential evapotranspiration assessment methods for hydrological modelling with SWAT—Application in data-scarce rural Tunisia, Agricultural Water Management, 174, 39–51, https://doi.org/10.1016/j.agwat.2016.03.004, 2016.

Bai, P., Liu, X., Yang, T., Li, F., Liang, K., Hu, S., and Liu, C.: Assessment of the Influences of Different Potential Evapotranspiration Inputs on the Performance of Monthly Hydrological Models under Different Climatic Conditions, Journal of Hydrometeorology, 17, 2259–2274, https://doi.org/10.1175/JHM-D-15-0202.1, 2016.

Berghuijs, W. R., Larsen, J. R., van Emmerik, T. H. M., and Woods, R. A.: A Global Assessment of Runoff Sensitivity to Changes in Precipitation, Potential Evaporation, and Other Factors, Water Resources Research, 53, 8475–8486, https://doi.org/10.1002/2017WR021593, 2017.

Birhanu, D., Kim, H., Jang, C., and Park, S.: Does the Complexity of Evapotranspiration and Hydrological Models Enhance Robustness?, Sustainability, 10, 2837, https://doi.org/10.3390/su10082837, 2018.

Boeing, F., Wagener, T., Marx, A., Rakovec, O., Kumar, R., Samaniego, L., and Attinger, S.: Increasing influence of evapotranspiration on prolonged water storage recovery in Germany, Environmental Research Letters, 19, 024 047, https://doi.org/10.1088/1748-9326/ad24ce, 2024.

Bruno, G. and Duethmann, D.: Increases in Water Balance-Derived Catchment Evapotranspiration in Germany During 1970s–2000s Turning Into Decreases Over the Last Two Decades, Despite Uncertainties, Geophysical Research Letters, 51, e2023GL107 753, https://doi.org/10.1029/2023GL107753, 2024.

Devia, G. K., Ganasri, B., and Dwarakish, G.: A Review on Hydrological Models, Aquatic Procedia, 4, 1001–1007, https://doi.org/10.1016/j.aqpro.2015.02.126, 2015.

Guo, D., Westra, S., and Maier, H. R.: Sensitivity of potential evapotranspiration to changes in climate variables for different Australian climatic zones, Hydrology and Earth System Sciences, 21, 2107–2126, https://doi.org/10.5194/hess-21-2107-2017, 2017.

Hanselmann, N., Osuch, M., Wawrzyniak, T., and Alphonse, A. B.: Evaluating potential evapotranspiration methods in a rapidly warming Arctic region, SW Spitsbergen (1983–2023), Journal of Hydrology: Regional Studies, 56, 101 979, https://doi.org/10.1016/j.ejrh.2024.101979, 2024.

Hua, D., Hao, X., Zhang, Y., and Qin, J.: Uncertainty assessment of potential evapotranspiration in arid areas, as estimated by the Penman-Monteith method, Journal of Arid Land, 12, 166–180, https://doi.org/10.1007/s40333-020-0093-7, 2020.

Jung, I. W., Chang, H., and Risley, J.: Effects of runoff sensitivity and catchment characteristics on regional actual evapotranspiration trends in the conterminous US, Environmental Research Letters, 8, 044 002, https://doi.org/10.1088/1748-9326/8/4/044002, 2013.

Kuentz, A., Arheimer, B., Hundecha, Y., and Wagener, T.: Understanding hydrologic variability across Europe through catchment classification, Hydrology and Earth System Sciences, 21, 2863–2879, https://doi.org/10.5194/hess-21-2863-2017, 2017.

Liu, Y., Jiang, Q., Wang, Q., Jin, Y., Yue, Q., Yu, J., Zheng, Y., Jiang, W., and Yao, X.: The divergence between potential and actual evapotranspiration: An insight from climate, water, and vegetation change, Science of The Total Environment, 807, 150 648, https://doi.org/10.1016/j.scitotenv.2021.150648, 2022.

Lu, J., Sun, G., McNulty, S. G., and Amatya, D. M.: A COMPARISON OF SIX POTENTIAL EVAPOTRANSPIRATION METHODS FOR REGIONAL USE IN THE SOUTHEASTERN UNITED STATES, Journal of the American Water Resources Association, 41, 621–633, https://doi.org/10.1111/j.1752-1688.2005.tb03759.x, 2005.

Massari, C., Avanzi, F., Bruno, G., Gabellani, S., Penna, D., and Camici, S.: Evaporation enhancement drives the European water-budget deficit during multi-year droughts, Hydrology and Earth System Sciences, 26, 1527–1543, https://doi.org/10.5194/hess-26-1527-2022, 2022.

Mazzoleni, M., Brandimarte, L., and Amaranto, A.: Evaluating precipitation datasets for large-scale distributed hydrological modelling, Journal of Hydrology, 578, 124 076, https://doi.org/10.1016/j.jhydrol.2019.124076, 2019.

Maček, U., Bezak, N., and Šraj, M.: Reference evapotranspiration changes in Slovenia, Europe, Agricultural and Forest Meteorology, 260-261, 183–192, https://doi.org/10.1016/j.agrformet.2018.06.014, 2018.

Ndiaye, P. M., Bodian, A., Dezetter, A., Ogilvie, A., and Goudiaby, O.: Sensitivity of global hydrological models to potential evapotranspiration estimation methods in the Senegal River Basin (West Africa), Journal of Hydrology: Regional Studies, 53, 101 823, https://doi.org/10.1016/j.ejrh.2024.101823, 2024.

Oudin, L., Michel, C., and Anctil, F.: Which potential evapotranspiration input for a lumped rainfall-runoff model?, Journal of Hydrology, 303, 275–289, https://doi.org/10.1016/j.jhydrol.2004.08.025, 2005.

Pfeifroth, U., Sanchez-Lorenzo, A., Manara, V., Trentmann, J., and Hollmann, R.: Trends and Variability of Surface Solar Radiation in Europe Based On Surface- and Satellite-Based Data Records, Journal of Geophysical Research: Atmospheres, 123, 1735–1754, https://doi.org/10.1002/2017JD027418, 2018.

Pimentel, R., Arheimer, B., Crochemore, L., Andersson, J. C. M., Pechlivanidis, I. G., and Gustafsson, D.: Which Potential Evapotranspiration Formula to Use in Hydrological Modeling World-Wide?, Water Resources Research, 59, e2022WR033 447, https://doi.org/10.1029/2022WR033447, 2023.

Reaver, N. G. F., Kaplan, D. A., Klammler, H., and Jawitz, J. W.: Theoretical and empirical evidence against the Budyko catchment trajectory conjecture, Hydrology and Earth System Sciences, 26, 1507–1525, https://doi.org/10.5194/hess-26-1507-2022, 2022.

Seiller, G. and Anctil, F.: How do potential evapotranspiration formulas influence hydrological projections?, Hydrological Sciences Journal, 61, 2249–2266, https://doi.org/10.1080/02626667.2015.1100302, 2016.

Shi, L., Wang, B., Liu, D. L., Feng, P., Cleverly, J., Li, L., Zhang, G., and Yu, Q.: Performance of potential evapotranspiration models across different climatic stations in New South Wales, Australia, Journal of Hydrology: Regional Studies, 50, 101 573, https://doi.org/10.1016/j.ejrh.2023.101573, 2023.

Teuling, A. J., de Badts, E. A. G., Jansen, F. A., Fuchs, R., Buitink, J., Hoek van Dijke, A. J., and Sterling, S. M.: Climate change, reforestation/afforestation, and urbanization impacts on evapotranspiration and streamflow in Europe, Hydrology and Earth System Sciences, 23, 3631–3652, https://doi.org/10.5194/hess-23-3631-2019, 2019.

Thornthwaite, C. W.: An Approach toward a Rational Classification of Climate, Geographical Review, 38, 55, https://doi.org/10.2307/210739, 1948.

Voisin, N., Wood, A. W., and Lettenmaier, D. P.: Evaluation of Precipitation Products for Global Hydrological Prediction, Journal of Hydrometeorology, 9, 388–407, https://doi.org/10.1175/2007JHM938.1, 2008.

Wang, J., Zhuo, L., Han, D., Liu, Y., and Rico-Ramirez, M. A.: Hydrological Model Adaptability to Rainfall Inputs of Varied Quality, Water Resources Research, 59, e2022WR032 484, https://doi.org/10.1029/2022WR032484, 2023.

Xiang, K., Li, Y., Horton, R., and Feng, H.: Similarity and difference of potential evapotranspiration and reference crop evapotranspiration – a review, Agricultural Water Management, 232, 106 043, https://doi.org/10.1016/j.agwat.2020.106043, 2020.

Zhang, D., Liu, X., Zhang, Q., Liang, K., and Liu, C.: Investigation of factors affecting intra-annual variability of evapotranspiration and streamflow under different climate conditions, Journal of Hydrology, 543, 759–769, https://doi.org/10.1016/j.jhydrol.2016.10.047, 2016.

Zhao, L., Xia, J., Xu, C.-y., Wang, Z., Sobkowiak, L., and Long, C.: Evapotranspiration estimation methods in hydrological models, Journal of Geographical Sciences, 23, 359–369, https://doi.org/10.1007/s11442-013-1015-9, 2013.